



NLR-TP-2000-061

## **Diagnosis of water motion in the Sloshsat FLEVO tank**

J.P.B. Vreeburg



NLR-TP-2000-061

## **Diagnosis of water motion in the Slososat FLEVO tank**

J.P.B. Vreeburg

This report is based on a presentation held at the 50<sup>th</sup> International Astronautical Congress, Amsterdam, the Netherlands, 4 - 8 October 1999.

The contents of this report may be cited on condition that full credit is given to NLR and the author.

Division:	Space
Issued:	February 2000
Classification of title:	unclassified



**Contents**

<b>Introduction</b>	3
<b>The Coarse Sensor Array, CSA</b>	4
<b>The NTC Anemometer</b>	5
<b>Conclusions</b>	8
<b>Acknowledgements</b>	8
<b>References</b>	8

6 Figures

## DIAGNOSIS OF WATER MOTION IN THE SLOSHSAT FLEVO TANK

JPB Vreeburg,  
National Aerospace Laboratory (NLR)  
PB 90502  
NL-1006 BM Amsterdam  
[vreeburg@nlr.nl](mailto:vreeburg@nlr.nl)

### Abstract

Sloshsat FLEVO is a spacecraft for the experimental study of liquid dynamics and liquid management problems in space. It is to be launched from a Hitchhiker bridge on the STS, and operated via the STS in its vicinity. The spacecraft is near completion. Of the total 110 kg mass of Sloshsat 33.5 kg is liquid water in a smooth 87 liter tank. The requirements on water quality drive the design of the Sloshsat tank and its instrumentation. All material in contact with the water must not be leached, be it by dissolution or electrolytic mechanisms. The distribution of the water in the tank is determined from the data of the Coarse Sensor Array, a uniform distribution of 45-mm rings over the inner surface of the tank. The rings are made from 0.5-mm platinum wire. The measurement is the electrical capacitance between adjacent rings, and is sensitive out to approx. 30 mm. The liquid flow is measured at 10 locations at a distance of 3 mm from the tank wall. There is located a 0.3 mm bead ntc that is operated as a thermal transient anemometer. At three locations, a Fine Height Sensor is installed to give a precise measurement of the liquid height. This data is required to support CSA data, and its rate of change is expected to diagnose capillary ripple. Tests gave confidence that a polyethylene tank lining, and sensors made from Pt-wire or glass would allow preserving the water quality through the pre-launch standing period and the orbital phase. Surface-active material is easily dissolved from glue and destroys surface tension while ions released by redox activity increase conductivity. The paper gives descriptions of the tank major instrumentation hardware, of the methods to validate the performances, and illustrations of calibration data that have been collected for interpretation of the measurements in the tank.

### Introduction

The presence of liquid, e.g. fuel, onboard spacecraft brings control problems that do not exist for completely rigid vehicles. The liquid cannot always be constrained in a completely full tank, and so may show large excursions in response to spacecraft maneuvering. The liquid motions are generally denoted by 'slosh' and have two important consequences. First, spacecraft control must reckon with the liquid force and torque on the tank wall, and the tank wall motion should not pump momentum into the liquid mass. Second, liquid often is required to be maintained above the tank exit and be without bubbles, a control activity denoted 'liquid management'. Although models exist for the prediction of liquid behaviour on spacecraft, their validation is problematic because some physical phenomena are poorly understood, e.g. the motion of the liquid at the liquid-solid contact line. The experimental program for Sloshsat FLEVO is designed to elucidate some of these problems (Vreeburg and Soo, 1998). A sketch of Sloshsat FLEVO is given as figure 1.

The instrumentation for the experiments with Sloshsat consists of a Motion Sensing Subsystem or MSS (Dujardin, 1998) and tank instrumentation. The MSS is constructed with three gyroscopes and six linear accelerometers. Its output data can be reconstructed to provide the force and torque that act on the rigid part of Sloshsat, an effective dynamometer configuration. The sensors in the tank give the data on the liquid distribution and flow field.

The tank shape is a circular cylinder with length equal to radius and with hemispherical ends. The size of the radius is 0.228 m which makes the tank volume 86.88 liters. The tank is smooth, except for some minor intrusions by sensors, and contains no structure, just 33.5 kg of water. Since the launch of Sloshsat is by STS, water turned out to be the only



polar liquid compatible with the safety requirements. The experiment liquid must have physical properties that stay constant. In particular the electric conductivity is to remain at a low value in order that the Coarse Sensor Array works as planned. The surface tension of the water should be at its high nominal value of 72 mN/m, or the Weber and Bond numbers during the experiments show unacceptably high values.

The requirements on water quality drive the design of the Sloshtank and its instrumentation. Tests gave confidence that a polyethylene tank lining and sensors made from Pt-wire would not degrade the essential capillary and electric properties during the pre-launch standing period and the orbital phase. The third material that had to be allowed was the glassy 0.3 mm bead that encloses the ntc sensors. In the sequel the two major tank instrumentation systems, CSA and anemometer set (10 sensors) will be presented. Not discussed are the Fine Height Sensor (FHS) and Conductivity Sensor (CS).

#### The Coarse Sensor Array, CSA

The Sloshtank Coarse Sensor Array consists of a nearly uniform distribution of 45 mm diameter rings made of platinum wire with diameter 0.5 mm. The 137 rings are mounted flush with the Sloshtank tank wall and provide a total of 270 pairs that allow among each the measurement of electrical capacitance. Figure 2a shows the installation of a ring on the tank core (after the tank has been build up, this aluminum core is dissolved by NaOH) and figure 2b shows some rings as seen through the porthole of the finished tank. The capacitance value is a measure of the amount of liquid between the rings, or, for a continuous liquid distribution, of the average liquid height between the rings. The normal vectors at midpoint locations of the 270 ring-pairs are shown in figure 3, together with the locations of the rings. If the water height is more than about 30 mm, the capacitance value is at its maximum, or saturated, and no additional information can be obtained.

The Coarse Sensor Array capabilities are determined by its capacitive sensing element, the ring-pair. It is a general property of adjacent capacitor plates of size  $D$  and spacing  $D$  that their capacitance value under a layer of dielectric liquid may increase with increasing liquid up to a height of magnitude  $D$ . Further increases do not give

additional change in capacitance. Liquid conductivity tends to compress the field, i.e. decreases the penetration depth. Since the field lines between the plates are concentrated at the edges, leaving out the center has little effect and so a wire ring was chosen. A benefit of the wire geometry is the constant curvature at the circumference of the ring.

The performance of the CSA, based on the above considerations was deemed acceptable since it could be expected to yield the approximate liquid geometry about the contact line region, at comparatively modest investment in data handling provisions. The array sampling frequency of 3 Hz and the discretization of the sensor output in 4 bits were chosen subsequently.

Electrical properties The conductivity of the water, in spite of the PE tank lining requires conditioning. The complex impedance of a ring-pair in contact with the water and as a function of frequency must be determined in order to design an appropriate measurement circuit. The solutions to these problems have been achieved with the help and counsel of different experts. The water conductivity was stabilized by adding some amount of 0.5 mm diameter pellets that are used as the active element in de-ionization loops. The equivalent circuit of a ring-pair in contact with the water was determined from Frequency Response Analyzer measurements. As it turned out, about the 30 kHz sensor operation frequency, the equivalent circuit consists of a resistance of approximately 10 kOhm in series with a parallel resistance and capacitance pair (Metcalf, 1965). The resistance in the pair is about 800 kOhm for good quality water but may become as low as 100 kOhm without de-ionization pellets. The capacitance of the pair varies between 30-35 pF, with liquid height, or at a higher level for higher water conductance.

Calibration data The performance of the CSA in the flight tank is determined with 5 kg of water. On earth this amount gives a maximum water height of about 7 cm, well into the saturation value for the ring-pair. However, the ring-pairs near the liquid-tank contact line have less water over them and so should give values below saturation. The configuration of the water in the tank depends on the elevation of the tank centerline. A Matlab



program was written for the liquid geometry with respect to the CSA. An illustration is given in figure 4a.

At this time of writing the calibration measurements have not yet been concluded so no full information on the results can be given. A preliminary data set is shown in figure 4b for a vertical centerline. Each measured value is plotted at the midpoint between the rings. The magnitude of the data is reflected in the size of the marker. Note that a near contact line position appears to increase the measurement value.

The calibration program calls for different attitudes and orientations of the tank. The different configurations are separated by 10 degrees in elevation of the tank centerline, or in roll angle about the centerline. Hence, altogether  $17 \times 36 + 2$  configurations need to be measured. At vertical centerline, roll does not bring different configuration, whence the 2 in the summation of cases to be evaluated. Liquid motion has been found not to affect the measurement, other than its effect on the liquid geometry. The temperature of the water does have an effect on the magnitude of the capacitance value.

From the calibration data set it is intended to determine weight factors for measurements by individual ring-pairs. The weight factor is to correct for differences in sensitivity, due to differences in material and electrical environments.

#### The NTC Anemometer

The anemometer should be capable to measure liquid velocity in the range 0 to 100 mm/s with a resolution of 1 mm/s near the no-flow state and a resolution of 5 mm/s near the 100 mm/s value.

Commercially available flow anemometers that had appropriate specifications for application in the Sloshsat tank were not found, not even in the medical field. It was therefore decided to operate the negative temperature coefficient (ntc) temperature sensors also as anemometer.

The Anemometer Configuration The ntc sensor is a small bead type: 111-202CAK-B01, manufactured by Fenwall Electronics. It sits on top of a conical pedestal that extends in a cylindrical solid of

polyethylene, the same material as the Sloshsat experiment tank. This part contains a platinum heating wire to melt the cylinder after it has been placed in a matching hole in the experiment tank. The melted PE fuses the material of cylinder and tankwall to achieve a leak-free integration of the sensor in the tank. Figure 5 gives a picture of the sensor before its pedestal is covered with PE.

The approximate diameter of the ntc sensor bead is 0.3 mm. The height of the cone from its base on the tank wall is about 3 mm. Consequently the Reynolds number based on bead dimension is about 30 at maximum flow velocity, and proportionally higher near the wall. The value of the Reynolds number is important for the prediction of the flow regime. To be feared is intermittent flow induced by the geometry of the sensor since this will give strong measurement oscillations and a bad value for the ambient flow velocity. The steady flow about a free sphere (and all other simple bodies) shows a steady wake with dimension less than the size of the sphere for a Reynolds number up to about 100 [Clift, Grace and Weber, 1978]. Consequently, in steady flow a monotonous behaviour of the heat transfer coefficient is to be expected for the full velocity range in Sloshsat. The cone is not expected to change the monotonous character of the flowfield: although the size of the base is much larger than the bead diameter, the flow velocity near the base will be much smaller and so the Reynolds number could not increase very much, if at all. If the sensor mount is considered to be a cylinder, the oscillatory flow regime starts for Reynolds number more than about 100 (von Karman vortex street), a value already considered to be a safe upper limit.

Measurement theory The ntc anemometer is based on a transient response measurement [Bailey et al, 1993]. The theory predicts the temperature of the ntc to adjust to the ambient temperature according to a single exponential [Tychonov and Samarski, 1963]:

$$T(t) \sim T_e + A \cdot \exp(-Fo \cdot x^2 \cdot t)$$

where  $T(t)$  = the temporal value of the ntc temperature

$T_e$  = the final equilibrium temperature of the ntc

$A$  = a constant value

$Fo$  = the Fourier number for the system

$x$  = the smallest eigenvalue of the configuration

$t$  = time

In order to size the ntc and its operational parameters, an analysis of the system has been made. The ntc is modelled as a sphere with two regions of contact conductance, or, two regions with a different Biot number. One of the Biot numbers is constant since it represents the conductance to the ntc base. The other Biot number is variable; it depends on the heat flow to and convected by the liquid and so is related to the liquid velocity at the ntc. The results of the analysis gave the functional dependence of the temperature decay on the different parameters, and was used to optimize the system. The best operational mode has been determined empirically.

Sensor operation The ntc is operated within the constraints of the Slosat onboard time discretizations at 3 Hz and 30 Hz. Each ntc is activated periodically on a basis of 20 steps of 33 ms, or, each ntc gives 3 velocity measurements every 2 s. In the first 33 ms of the period a 2.5 mA current heats the ntc about 20 K above ambient. Then for two 33 ms increments the ntc is left to stabilize the decay phenomenon. The next 6 steps of 33 ms the ntc temperature is measured with a 0.25 mA current. These data are used to determine the exponential decay coefficient, the constant  $A$  that multiplies the exponential and the constant equilibrium value of the temperature  $T_e$ , thus altogether 3 parameters. During initial testing ntc temperature data were taken at 1000 Hz, and it was found that the decay curve came very close to the temperature equilibrium value after about 300 ms. This is in accordance with the characteristic time for the ntc that follows from a value 1 of the Fourier number of the system.

Data reduction algorithms For each velocity determination six data are taken. The theoretical expression that relates the measurement to the flow has three parameters so the data processing problem is overdetermined. This allows to process in a least-squares mode and thereby obtain robustness against noise errors.

The standard processing recovers the three unknown parameters from a Prony algorithm [Hildebrand, 1974] that acts on five measurement data taken consecutively, starting at 99 ms since the end of the heating pulse to the ntc. Hence, the first data, at 66 ms, of the full sequence is disregarded. Special processing may start with this data and use all six or some other scheme can be chosen. It has been found that there is some advantage in processing the first five of the six data when velocity is low. Although the parameters are determined by a least-squares scheme, the deviations at each data point do not have equal effects on the resulting parameter values. The Prony algorithm weighs the first data more than the last. Consequently there is a different result when the data are processed in reverse order and such approach has been found useful for the reduction of spread at low velocity measurements.

A distinct feature of Prony algorithms is the equal spacing between consecutive measurements. An alternative scheme without this restriction has been tried also. The method is to take the logarithm of the exponential in the expression for the temperature behaviour and match the resulting values least-squares to a straight line. However, before the logarithm can be determined one must know the equilibrium temperature value  $T_e$ . An advantage of the Prony algorithm is that this value is obtained from the data. In order to compare the alternative scheme with the standard Prony, the equilibrium temperature as determined by Prony was used to obtain the exponential. The result of the comparison has been that the two methods give comparable results for good data sequences, but the Prony method is superior for data with large errors. The comparison was performed with data taken at 1000 Hz and so an accurate plot of the temperature decay could be generated.

Although the initial plan had been to use the decay exponent as a measure for the velocity, it turned out that the coefficient of this exponential (the value of  $A$  in the function representation) promises better data. Its range spanned from 1 near 100 mm/s to 3 near zero velocity, the change is approximately proportional to the velocity change (but the sensitivity is largest at zero velocity), and the value proved to be quite insensitive to errors in the sequence of data. The best performance, as quoted in the previous sentence, is obtained again with the

last five data from the sequence of six. The theory relates this coefficient to the initial temperature field in the ntc in absence of heating pulse, but with measurement current. A comparable, although different, sensor principle [Sonnenschmidt and Vanselow, 1996] was found to use also the coefficient(s) rather than the decay exponent as the measurement variable.

Calibration set-up One of the early findings in working with the ntc has been that the directionality of the anemometer is small, and will not seriously degrade the measurement of the magnitude of the flow velocity vector. Another, that the ntc does not become dangerously overheated by the heating pulses when it is outside the liquid.

The relevant tests have been done in a transient laminar pipe flow, generated by flushing a reservoir. The pipe has length 0.335 m and an inner diameter of 19 mm. It is mounted vertically under a conical spout that matches a reservoir to the pipe. The exit of the pipe is connected to a tube with a valve to start the liquid flow. The tube ends in a collector vessel that is placed on an electronic scales for the measurement of the transported liquid mass. For all cases, the collected mass has been read once per second. From the collector, a pump takes the water through a thermostat and back to the reservoir on top of the pipe.

Ntc anemometers can be mounted at four locations symmetrically disposed at a cross-section of the pipe 0.237 m from the entrance, i.e. at a distance of about 12 diameters. When installed in the pipe, the ntc is at 3 mm from the wall (as it will be in the Sloshsat tank), or about at station  $0.7 r$ , where  $r$  is the radius of the pipe. It has been established that in the entrance region of a stationary pipe flow the velocity at this station is approximately equal to the average flow in the pipe [Smith, 1960]. But, that velocity profile is not necessarily relevant to the flow in the calibration set-up and further discussion is required, even if possible distortion of the velocity profile from blockage of the cross-section by the sensors is disregarded.

The flow through the pipe is transient, and the first, accelerated, part is governed by the opening rate of the valve. The valve was opened by hand and therefore not in a reproducible manner. However,

after some trials, the mass flow rate could be controlled to be fairly symmetrical to the rate in the decelerating part of the profile: the free flow from the reservoir. The maximum mass flow rate was calculated to be about 100 mm/s, which gives a Reynolds number based on pipe diameter of 2000.

Data on transient pipeflow are scarce. In a uniformly accelerated flow, the velocity profile across the pipe is found to be very flat [Kato et al, 1980]. Although the flow in the pipe had fairly constant acceleration and deceleration rates it was felt to be more justifiable to consider oscillatory flow results for the assessment of its profile. Oscillatory flow necessarily passes through zero velocity values (although these passes do not occur in phase across the cross-section), as at the opening of the valve and the emptying of the reservoir. From the behaviour of the uniformly accelerated flow one may surmise that the maximum velocity at the ntc is about equal to the maximum mass flow rate, when the flow starts to decelerate.

If the total flow history through the pipe is taken to be half a period in an oscillating flow, the duration of the period can be calculated and then also the Stokes (or Womersley) parameter,  $k$ , that has been

found relevant for these flows. Define  $k = r \sqrt{\frac{\omega}{\nu}}$ ,

where  $\omega$  = angular frequency of oscillation and  $\nu$  = kinematic viscosity, then  $k \sim 3$ , a fairly low value that corresponds to a thick boundary layer. It can be shown that station  $0.7 r$  is inside and near the edge of the boundary layer.

In [Eckmann and Grotberg, 1991] data for oscillatory water flows are discussed. These come from measurements by laser-Doppler, and by hot-wire anemometry, a method close to the ntc operation. The measured data do not include the present parameter pair  $Re = 2000$ ,  $k = 3$  but reference is made to earlier investigations on oscillatory air flow [Hino et al, 1976] that are applicable.

The conclusion is that the velocity as recorded at the ntc location has the same temporal development as the average velocity in the pipe, with some phase delay, for all flow rates except possibly the highest value. Here, near 100 mm/s, some turbulence may

develop at the start of the deceleration phase. This observation is in accordance with the data as taken during the calibration runs; some irregularities often occur in the calculated velocities at this transition.

Results A representative sequence of data from an anemometer in response to the transient pipe flow is given in figure 6c.

#### Conclusions

The tank instrumentation of Sloshtat FLEVO for the diagnosis of liquid velocity and flow field is based on simple sensors. Their use was mandated because of the necessary compatibility of the sensor material with pure water, for extended periods. Another factor that contributed to the system choice is the limited data collection, processing and transmission capability of a low-cost spacecraft like Sloshtat FLEVO.

The performance of the instrumentation is achieved by taking extensive data sets of the sensor response to liquid configurations on earth that are similar to configurations expected in space. Relatively sophisticated data processing algorithms are used to make the measurements robust against errors.

#### Acknowledgments

The sensor hardware was constructed by Wubbo de Grave of the NLR Space Department. He integrated the sensors and performed all measurements.

Sloshtat FLEVO is a harmonized programme between the European Space Agency (ESA) and the Netherlands Agency for Aerospace Programs (NIVR). Main contractor is the National Aerospace Laboratory NLR (The Netherlands) with participation of Fokker Space (The Netherlands), Verhaert (Belgium), Rafael (Israel) and NASA (USA). The Sloshtat FLEVO development is performed in the framework of the ESA Technology Development Programme (TDP) Phase 2 and the NIVR Research and Technology (NRT) programme.

#### References

1. Bailey, J.L., Vresk, J., Acharya, M., 'Evaluation of the performance characteristics of a thermal transient anemometer', *Exper. Fluids*, 15 (1993) 10-16.
2. Clift, R., Grace, J.R., Weber, M.E., 'Bubbles, Drops, and Particles', Academic, 1978.
3. Dujardin, P.G.J.P., 'Sloshtat FLEVO Motion Sensing Subsystem,' Proc. Workshop on Spacecraft Attitude and Orbit Control Systems, IFAC, ESA/Estec, Noordwijk, NL, 15-17 Sep. 1997. Also NLR TP 97451 U.
4. Eckmann, D., Grotberg, J.B., 'Experiments on transition to turbulence in oscillatory pipe flow', *J. Fluid Mech.*, 222 (1991) 329-350.
5. Hildebrand, F.B., 'Introduction to numerical analysis', 2<sup>nd</sup> ed., Dover, 1974.
6. Hino, M., Sawamoto, M., Takasu, S., 'Experiments on transition to turbulence in an oscillatory pipe flow', *J. Fluid Mech.*, 75 (1976) 2, 193-207
7. Kato, E., Suita, M., Kawamata, M., 'Visualization of unsteady pipe flows using hydrogen bubble technique', Proc. Intern. Symp. Flow Visualization Bochum, 9-12 Sep. 1988, Ruhr-Univ. Inst. Thermo-Fluiddyn., 342-346.
8. Metcalf, W.S., 'Measurement of conductance and dielectric constant of liquids by a.c. methods', *J. Sci. Instrum.* 42 (1965) 742-743.
9. Smith, A.M.O., 'Remarks on transition in a round tube', *J. Fluid Mech.*, 6 (1960) 565-576.
10. Sonnenschmidt, D., Vanselow, K.H., 'Measurement of water flow velocity by analysis of short temperature steps', *Meas. Sci. Technol.*, 7 (1996) 1536-1539.
11. Tychonov, A.N., Samarski, A.A., 'Partial Differential Equations of Mathematical Physics', Vol.2, Holden-Day, 1967.
12. Vreeburg, J.P.B., Soo, D.N., eds., Proc. Symp. 'Colloquium on Sloshtat and Liquid Dynamics in Spacecraft', Noordwijk, NL, Nov. 16-17, 1998, ESA WPP 158.

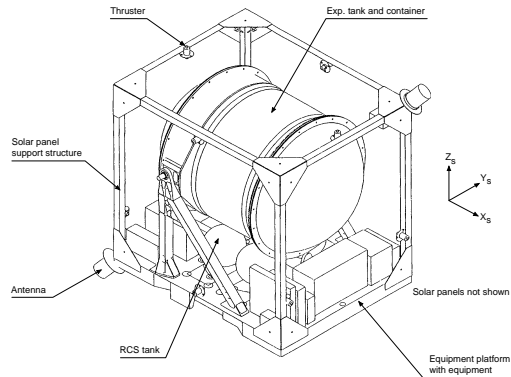


Fig. 1 Sketch of the Sloshtat FLEVO spacecraft

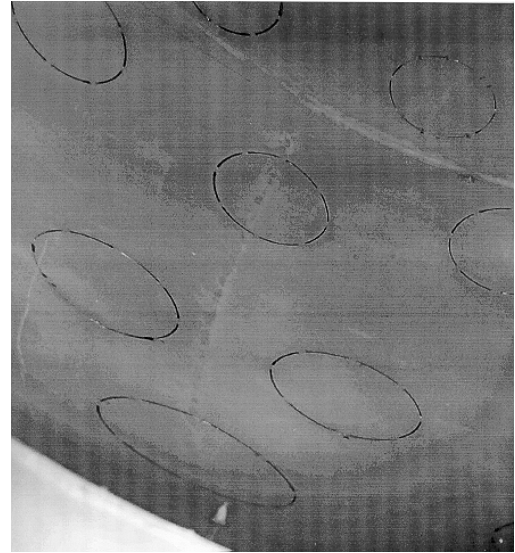


Fig. 2b View of tank wall with embedded rings



Fig. 2a Installation of a CSA ring on the tank core

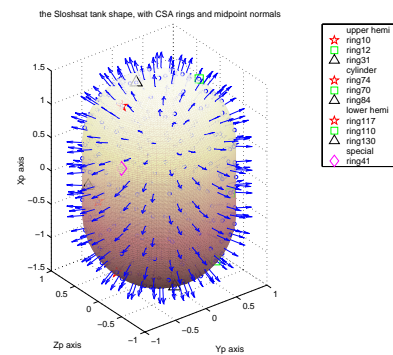


Fig. 3 Tank shape with CSA ring locations and pair midpoint normal vectors

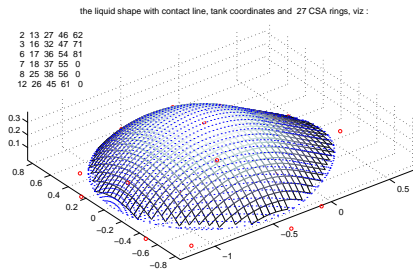


Fig. 4a Inclined tank with 5 kg of water and ring identifications

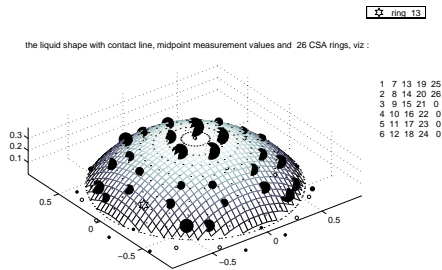


Fig. 4b Vertical tank with 5kg of water. The magnitude of each measurement value is represented by the marker size at the midpoint location

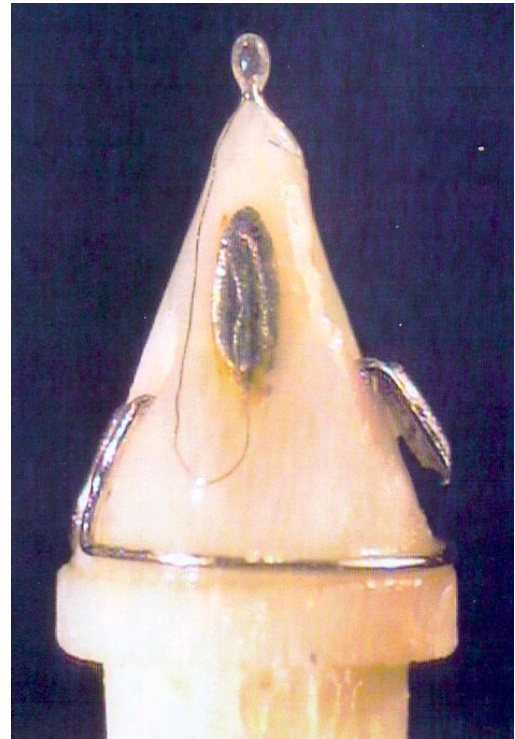


Fig. 5 The bare NTC anemometer

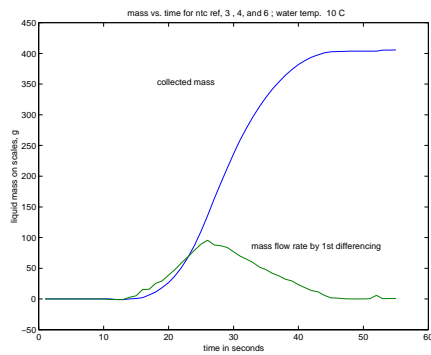


Fig. 6a The flushed water mass on the scales, and the mass flow rate, vs. time

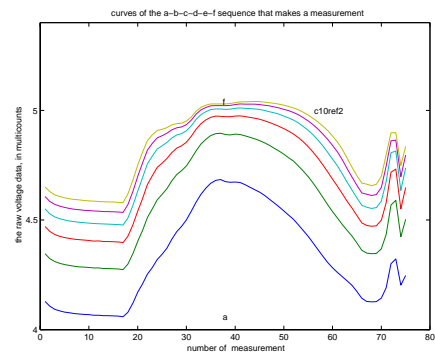


Fig. 6c The ntc sequence of 6 measurements, spaced by 33 ms, that are used to obtain data A as a measure of velocity.

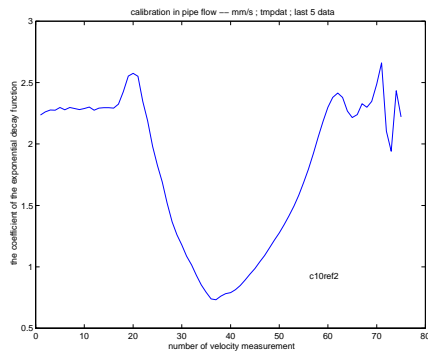


Fig. 6b The value of constant A in the expression for the ntc temperature, per measurement sequence of 6 data, determined by the Prony algorithm. Measurements are spaced with 2/3 seconds